



## Characteristics and simulation of soluble microbial products in membrane bioreactors coupled with moving carriers (MBR-MC)

Lin Chen<sup>a,\*</sup>, Chuqing Cao<sup>b</sup>

<sup>a</sup>School of Municipal and Environmental Engineering, Harbin Institute of Technology, Harbin, 150090, China  
Tel. +86-451-86418283; Fax: +86-451-86418283; email: hitlinchen@126.com

<sup>b</sup>School of Mechatronics Engineering, Harbin Institute of Technology, Harbin, 150090, China

Received 30 November 2010; Accepted 17 October 2011

### ABSTRACT

In this study, three lab-scaled membrane bioreactors (MBRs) coupled with moving carriers (MC) were operated under different sludge retention times (SRTs = 10, 30 and 50 d) for the treatment of synthetic wastewater. The characteristics of soluble microbial products (SMP) at each SRT were examined. The concentration of SMP in the supernatant firstly decreased from around 31.5 to 24.3 mg l<sup>-1</sup> when the SRT was increased from 10 to 30 d, and then showed a little increase as the SRT was further extended to 50 d. The profile of the molecular weight distribution (MWD) showed that the SMP had a wide spectrum of molecular weight. The dominant fraction with molecular mass higher than 10 kDa increased from 55.9% to 63.8% with the increase of the SRT from 10 to 50 d, while the two other fractions (1 kDa < MW < 10 kDa and MW < 1 kDa) subtly decreased. The excitation–emission matrix fluorescence spectroscopy (EEM) revealed that the SMP had three similar peak locations regardless of the SRT and the quenching effect of humic-like substance on protein should be considered. Response surface methodology was used to evaluate the effects of SRT, hydraulic retention time (HRT), temperature and aeration rate on the SMP production. The optimal parameters were obtained at an SRT of 33 d, an HRT of 10 h, a temperature of 19°C and an aeration rate of 1.5 m<sup>3</sup> h<sup>-1</sup>, giving rise to an SMP of 23.9 mg l<sup>-1</sup>. These results may serve as a useful guide for optimizing the operational parameters of the MBR-MC system to minimize the SMP production, and accordingly, improve the permeate quality and alleviate membrane fouling.

**Keywords:** Membrane bioreactor; Moving carrier; Soluble microbial products; Characteristics; Response surface methodology

### 1. Introduction

A conventional membrane bioreactor (MBR) is a system incorporating conventional activated sludge and microfiltration (or ultrafiltration) to achieve a complete solid–liquid separation independent of the characteristics of mixed liquor [1]. The advantages of an MBR over a conventional activated sludge (CAS) system have

been well reported such as excellent permeate quality, compact footprint, more concentrated biomass, reduced sludge yield and flexibility of operation [2]. Recently, an MBR coupled with moving carriers (MBR-MC) has been developed by several researchers [3,4], which was anticipated to achieve high simultaneous removal of nitrogen and to solve the poor settling problem of MBR. However, by their nature as filters, membrane fouling and its consequences in terms of operating costs limited the widespread application of MBR-MC.

\*Corresponding author.

In the application of MBR technology, soluble microbial products (SMP) are generally admitted to be the key foulants responsible for the long-term irreversible membrane fouling. It has been reported that SMP contributed 26%–52% of membrane fouling depended on the experimental conditions [5]. This tendency was confirmed by Rosenerger et al. [6], who found that the composition of liquid phase affected the filterability of activated sludge: an increase of SMP reduced the filtration index. Therefore, more detailed insights into the characteristics of SMP in MBRs were needed for understanding and controlling the membrane fouling.

The presence of SMP is also considered to be one of the important factors in biological wastewater treatment process, which affects the lower limit for treatment plants. Many experimental results also showed that only a small fraction of the soluble organic matter in the permeate was original influent substrate, while the majority of the soluble organic matter was of microbial origin [7,8]. Although the contributions of SMP to the efficient of the treatment [9] and the evolution of fouling in MBRs have been widely studied [10], few reports were available on the MBR-MC process.

The production of SMP involved a very complex process with many influential factors, such as sludge retention times (SRT), hydraulic retention time (HRT), temperature, dissolved oxygen (DO) concentration, substrate concentration, aeration rate etc. [4,7]. Therefore, it was necessary to select a criterion for the evaluation of the SMP production and to choose the optimum conditions. In conventional experiments, optimization was usually carried out by varying a single factor while keeping other factors fixed at a specific set of conditions. It was not only time-consuming, but also incapable of reaching the true optimal value due to ignoring the interactions among variables. Over the last decades, new techniques, such as response surface methodology (RSM), back propagation-genetic algorithm (BP-GA) and adaptive neuro-fuzzy inference system (ANFIS), have been used as efficient alternative tools for modeling of complex systems and widely used for forecasting. The use of RSM has been emphasized which is a combination of mathematical and statistical techniques aimed at evaluating the effects of several factors and searching optimum conditions for desirable responses. Since many operating variables were involved in the SMP formation, RSM can be employed as an appropriate approach to analyze the SMP formation process by varying them simultaneously and performing a limited number of experiments.

The objective of this study was to investigate the changes of SMP characteristics caused by different SRTs (SRTs = 10, 30 and 50 d). Molecular weight distribution

(MWD) and 3D excitation–emission matrix (EEM) fluorescence spectroscopy were applied to determine the characteristics of SMP, which could help to comprehend the production of SMP. Additionally, this study was also focused on the optimization of the SMP production with the RSM.

## 2. Materials and methods

### 2.1. Lab-scale setup and operation

Three laboratory-scale aerobic 150 l Plexiglass MBR-MC systems were used for the purpose of this study. Hollow-fiber microfiltration membranes with a pore size of 0.2  $\mu\text{m}$  and a surface area of 1  $\text{m}^2$  were used. The bio-cubes ( $2 \times 2 \times 2 \text{ cm}^3$ ) were mixed with suspended microorganisms in the reactor at a packing ratio of 5%. The synthetic wastewater was continuously introduced at an influent flow rate controlled by the liquid level in the reactor. The nutrient composition as the feed wastewater is listed in Table 1. The idle-filtration times switch ratio was set to 8 min: 2 min. Gas was diffused into the reactor through the air diffuser installed beneath the membrane module to maintain desired DO concentration, to control membrane fouling by hydraulic shear force and to circulate the porous media in the bioreactor. The sludge wasting volumes of each reactor corresponded to 15, 5, 3  $\text{l d}^{-1}$  for SRTs 10, 30, 50 d. In the different experimental runs, the sludge in the MBR-MC system was maintained at a steady state for one to two SRTs. The operation was stopped when the TMP reached 45 kPa, and then chemical cleaning was applied using 5% chlorine solutions for 2–8 h.

Table 1  
Composition of synthetic wastewater

Content	Concentration ( $\text{mg l}^{-1}$ )
Starch	171
Glucose	171
Urea	63.1
$\text{NaHCO}_3$	254.4
$\text{MgSO}_4$	42.9
$\text{CaCl}_2$	13.1
$\text{Fe SO}_4 \cdot 7\text{H}_2\text{O}$	4.2
$\text{MnCl}_2 \cdot 4\text{H}_2\text{O}$	0.3
$\text{ZnSO}_4 \cdot 7\text{H}_2\text{O}$	0.4
$\text{CuSO}_4 \cdot 5\text{H}_2\text{O}$	0.4
$\text{CoCl}_2 \cdot 6\text{H}_2\text{O}$	0.5

## 2.2. Analytical methods

The influent, mixed liquor and permeate were sampled three times per week and analyzed, evaluating mixed liquid volatile suspended solids (MLSS), COD,  $\text{NH}_4^+\text{-N}$ , total nitrogen (TN) and SMP. Except SMP, other chemical analyses were carried out according to Standard Methods [11]. Analysis of SMP in biomass suspensions collected from the MBR-MC was carried out after suspensions had been filtered with a 0.45  $\mu\text{m}$  filter. The phenol-sulfuric acid method [12] and the Lowry method [13] were used to determine the concentrations of carbohydrates and proteins, respectively. The concentration of SMP was calculated from the equation as follows [14]:

$$\text{Total SMP (as COD)} = 1.5 \text{ Proteins} + 1.07 \text{ Carbohydrates} \quad (1)$$

The MWD of the organic matters in SMP was determined using a GPC (Agilent 1100, Agilent) with a refractive index detector. The EEM spectra (FP 6500, JASCO) were collected with corresponding scanning emission spectra from 220 to 600 nm at 2 nm increments by varying the excitation wavelength from 220 to 420 nm at 5 nm sampling intervals. Particle size distribution of the mixed liquor was detected by a laser granulometer (Mastersizer 2000, Malvern).

## 2.3. Response surface methodology

The SRT, HRT, temperature and aeration rate were selected as independent factors, and the amount of SMP production was chosen as the response for the different processes. The range and levels used in the experiment were chosen taking into account our preliminary experiments (Table 2), in which  $X_1$  denoted SRT,  $X_2$  HRT,  $X_3$  temperature and  $X_4$  aeration rate, respectively. A second-order polynomial model by the response surface regression procedure that identified all of the possible interactions between the selected factors was as follows:

$$Y = b_0 + \sum_{i=1}^k b_i X_i + \sum_{i=1}^k b_i X_i^2 + \sum_{i < j} b_{ij} X_i X_j \quad (i = 1, 2 \dots j) \quad (2)$$

where  $Y$  = the response variable;  $b_0$ ,  $b_i$  and  $b_{ij}$  = the constant regression coefficients of the equation.

Two statistical indices were used to evaluate statistically accurate and valid predictions: coefficient of determination  $R^2$  and adjusted  $R^2$  by Eqs. (3) and (4), respectively.

$$R^2 = 1 - \frac{\sum_i (y_i - f_i)^2}{\sum_i (y_i - \bar{y})^2} \quad (3)$$

$$\text{Adjusted } R^2 = 1 - (1 - R^2) \frac{n - 1}{n - p - 1} \quad (4)$$

where  $\bar{y}$  is the mean of the observed data,  $y_i$  is the observed data,  $f_i$  is the predicted value,  $p$  is the total number of regressors in the linear model (but not counting the constant term) and  $n$  is the sample size.

The parameters of the response equations and corresponding analysis on variations were evaluated using Matlab 7.6 (The Math Work Inc., USA). The interactive effects of the independent variables on the dependent ones were illustrated by 3- and 2D contour plots.

## 3. Results and discussion

### 3.1. Performance of MBR-MC system under different SRTs

Table 3 shows the concentrations of COD, TN and  $\text{NH}_4^+\text{-N}$  in the influent and permeate at different SRTs. The average influent COD and TN over the entire period of operation were  $414.8 \pm 80.2$  and  $36.3 \pm 6.4 \text{ mg l}^{-1}$ , respectively. Nearly 98% of the organic substrate was removed by the MBR-MC treatment regardless of the operated SRT. The concentration of  $\text{NH}_4^+\text{-N}$  in the permeate was in the range of 0.6–1.6  $\text{mg l}^{-1}$  during the experiment. The higher rate of nitrification achieved at different SRTs can be attributed to the effective membrane retention of slow-growing nitrifying bacteria and the bacteria adherence to MC. Thus, the MBR-MC system was a reliable treatment process to realize the excellent pollutant removal.

### 3.2. Characteristics of SMP under different SRTs

SMP accumulation in a membrane system was heavily dependent on the operational parameters and the membrane properties. Fig. 1(a) demonstrates the concentration of SMP in the supernatant and permeate at different SRTs, which is indicated by Eq. (1). The concentration of SMP in the supernatant firstly decreased from around 31.5 to 24.3  $\text{mg l}^{-1}$  when the SRT was increased from 10 to 30 d, and then showed a litter increase to 27.2  $\text{mg l}^{-1}$  as the SRT was extended to 50 d. This result implied that the potential effect of SMP on system performances (e.g., membrane fouling) might be more striking at short and long SRTs. It was consistent with previous reports that there existed an optimum range of SRT for minimized the SMP production [7,15]. It can also be found that the concentration of SMP in the supernatant was always higher than that in the permeate, suggesting that some components of SMP were retained by the membranes. The retained SMP were utilized by heterotrophy or accumulated in

Table 2

Box-Behnken design matrix with four independent variables for the actual and predicted SMP production values

Run	Independent variable				Dependent variable						
	Coded values				Actual values				SMP production values (mg l <sup>-1</sup> )		
	X <sub>1</sub>	X <sub>2</sub>	X <sub>3</sub>	X <sub>4</sub>	X <sub>1</sub> (d)	X <sub>2</sub> (h)	X <sub>3</sub> (°C)	X <sub>4</sub> (m <sup>3</sup> h <sup>-1</sup> )	Experiment	Prediction (unreduced model)	Prediction (reduced model)
1	-1	-1	0	0	10	3	20	1.2	35.7	33.4	32.2
2	-1	1	0	0	10	13	20	1.2	32.8	30.8	32.2
3	1	-1	0	0	50	3	20	1.2	31.7	29.5	28.4
4	1	1	0	0	50	13	20	1.2	28.9	27.0	28.4
5	0	0	-1	-1	30	8	8	0.2	39.2	37.7	37.9
6	0	0	-1	1	30	8	8	2.2	36.2	33.0	32.6
7	0	0	1	-1	30	8	32	0.2	41.5	40.6	40.2
8	0	0	1	1	30	8	32	2.2	37.4	34.7	34.9
9	-1	0	0	-1	10	8	20	0.2	41.1	40.7	39.6
10	-1	0	0	1	10	8	20	2.2	31.5	33.3	34.3
11	1	0	0	-1	50	8	20	0.2	34.8	34.8	35.8
12	1	0	0	1	50	8	20	2.2	29.4	31.5	30.4
13	0	-1	-1	0	30	3	8	1.2	30.1	31.1	30.5
14	0	-1	1	0	30	3	32	1.2	33.8	34.6	32.8
15	0	1	-1	0	30	13	8	1.2	28.8	29.8	30.5
16	0	1	1	0	30	13	32	1.2	30.2	30.9	32.8
17	-1	0	-1	0	10	8	8	1.2	36.7	38.3	38.2
18	-1	0	1	0	10	8	32	1.2	39.2	40.5	40.5
19	1	0	-1	0	50	8	8	1.2	33.3	34.4	34.4
20	1	0	1	0	50	8	32	1.2	35.9	36.8	36.7
21	0	-1	0	-1	30	3	20	0.2	31.9	33.5	31.9
22	0	-1	0	1	30	3	20	2.2	26.2	27.3	26.6
23	0	1	0	-1	30	13	20	0.2	28.8	30.1	31.9
24	0	1	0	1	30	13	20	2.2	24.7	25.6	26.6
25	0	0	0	0	30	8	20	1.2	24.3	24.7	24.5
26	0	0	0	0	30	8	20	1.2	23.9	24.7	24.5
27	0	0	0	0	30	8	20	1.2	25.8	24.7	24.5

Table 3

COD and NH<sub>4</sub><sup>+</sup>-N concentration in MBR at different SRTs

SRT (d)	Influent COD (mg l <sup>-1</sup> )	Permeate COD (mg l <sup>-1</sup> )	Influent TN (mg l <sup>-1</sup> )	Permeate TN (mg l <sup>-1</sup> )	Permeate NH <sub>4</sub> <sup>+</sup> -N (mg l <sup>-1</sup> )
10		16.4 ± (8.7)		21.4 ± (4.6)	1.6 ± (0.3)
30	414.8 ± (80.2) <sup>1</sup>	14.4 ± (7.5)	40.4 ± (6.4)	19.8 ± (4.4)	0.4 ± (0.2)
50		17.3 ± (9.7)		17.3 ± (3.4)	0.6 ± (0.3)

<sup>1</sup>Standard deviation given in parentheses.Number of measurement for each SRT: *n* = 30.



the cake layer and membrane pores, leading to a relative stable concentration of SMP in the bulk phase.

The measurements of two major components of SMP—carbohydrates and proteins—are conducted as shown in Fig. 1(b). The concentration of carbohydrates and proteins in the supernatant showed the same tendency as that for SMP, which firstly decreased as the SRT was increased from 10 to 30 d and then increased with the further extension of SRT. Similarly, the concentration of carbohydrates and proteins in the supernatant was higher than that in the permeate, suggesting that carbohydrates and proteins were effectively intercepted by membrane and served as substrates for biomass growth. Additionally, the concentration of carbohydrates in the permeate increased from 6.9 to 8.5 mg l<sup>-1</sup> as the SRT was increased from 10 to 50 d. The concentration of proteins in the permeate also increased subtly from 2.6 to 4.2 mg l<sup>-1</sup>

when the SRT was extended from 10 to 50 d. Except the membrane properties and SMP characteristics, the effect of interceptions on the carbohydrates and proteins was also closely associated with the feature of the cake layer on the membrane surface. The mean particle size of sludge at 30–50 d SRT (SRT = 30 d:  $D_{50}$  = 59.5  $\mu$ m; SRT = 50 d:  $D_{50}$  = 62.4  $\mu$ m) was larger than that at 10 d SRT ( $D_{50}$  = 39.9  $\mu$ m). The cake layer constructed with large particles enabled to have a relative higher porosity than that with small particles [16], which might be a possible cause leading to a litter increase of carbohydrates and proteins in the permeate at 30–50 d SRT compared with 10 d SRT.

### 3.3. Molecular weight distribution of SMP at different SRTs

The molecular weight distribution of SMP was measured and compared under different SRTs, comprising a variety of components with a broad spectrum of molecular weights. In order to better understand MW distributions, the fractionations of MW > 10 kDa, 1 kDa < MW < 10 kDa and MW < 1 kDa were calculated (Fig. 2). The dominant fraction of higher than 10 kDa increased from 55.9% to 63.8% with the increase of SRT from 10 to 50 d, while the two other fractions subtly decreased. The SMP with a molecular weight lower than 1 kDa only constituted a small amount of SMP from 10.1% (SRT = 50 d) to 14.1% (SRT = 10 d). The MWD in the range between 1 kDa and 10 kDa constituted a second amount of SMP from 26.2% (SRT = 50 d) to 30.0% (SRT = 10 d). This result was in consistent with previous study [17] focused on conventional MBR, which showed the apparent molecular weight distributions of MBR supernatant at different SRTs and observed a smaller fraction

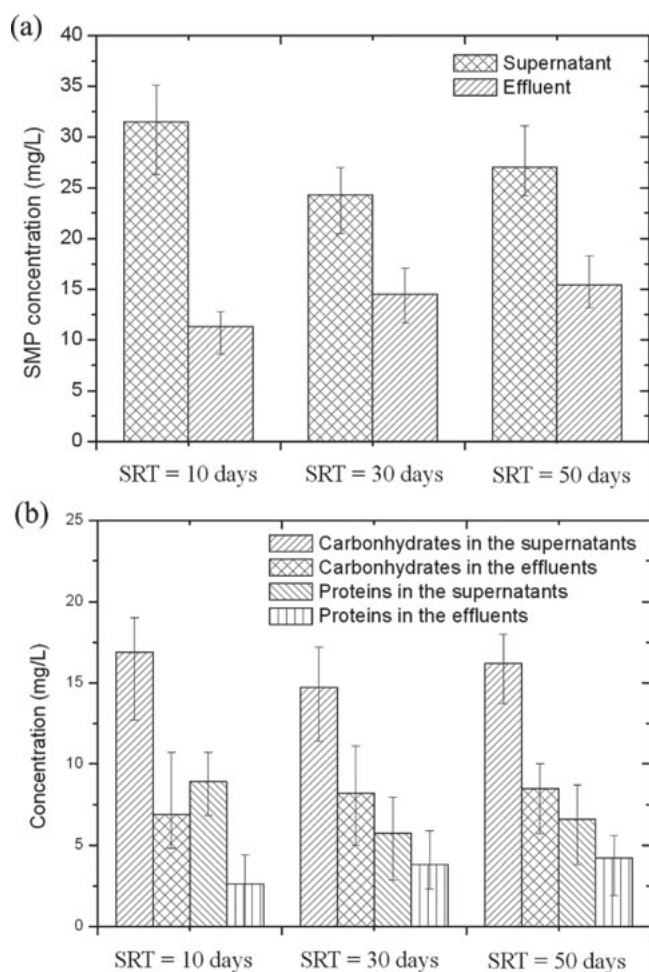


Fig. 1. Concentration of SMP in the three MBR-MC systems. (a) Total concentration of SMP in the supernatant and permeate at different SRTs. (b) Carbohydrates and proteins concentrations in the supernatant and permeate at different SRTs (HRT = 8 h; temperature = 20°C; aeration rate = 1.2 m<sup>3</sup> h<sup>-1</sup>).

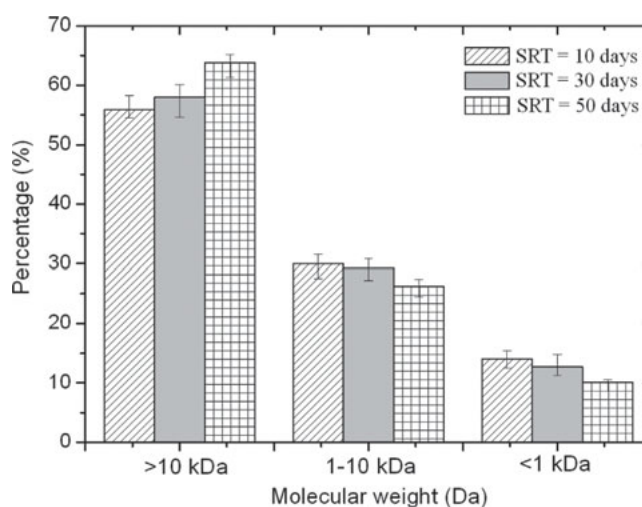


Fig. 2. Molecular weight distributions of SMP in the supernatant at different SRTs.

of small molecules but larger fractions of intermediate and large molecules. Barker and Stuckey [7] also found that the molecular weight distribution of SMP was greatly affected by SRT with large molecular weight components became more evident at long SRTs.

SMP can be classified into two groups based on the bacterial phase from which they are derived: the utilization-associated products (UAP) associated with substrate degradation and the biomass-associated products (BAP) generated in the endogenous phase. The UAP were found to be carbonaceous compounds with a MW lower than BAP which were mainly cellular macromolecules with an MW in a range of 290–5000 kDa [18]. There was an increase in BAP concentration and a simultaneous decrease in UAP concentration as the SRT was extended [15], thus leading to an increment of large molecules fractions.

### 3.4. EEM fluorescence spectra measured for SMP

Using consistent excitation and emission wavelength boundaries for EEM, five regions could be defined based on previous literature [19], including simple aromatic proteins such as tyrosine, aromatic proteins such as tryptophan, soluble microbial byproduct, humic acid-like materials and fulvic acid-like materials.

Measurements of the 3D EEM fluorescence spectra of SMP under different SRTs (10, 30 and 50 d) are carried out as shown in Fig. 3. In the three EEM maps, three main peak locations could be easily identified in the three SMP samples with no difference, at the excitation/emission wavelengths (Ex/Em) of 270/350, 340/420 and 250/450 nm. The three peaks could be attributed to soluble microbial byproduct, humic acid-like and fulvic acid-like substances, respectively. However, no peak representing the tyrosine protein-like and tryptophan protein-like substances was appeared in the fluorescence spectra of SMP at 10–50 d SRTs, which apparently suggested that the concentration of proteins in SMP was nearly zero. This result of fluorescence observation was obviously contrasted with the experimental results (Fig. 1(b)), which might be related with the quenching effect. Quenching refers to any process which decreases the fluorescence intensity of a given substance. In order to assess the extension of the quenching effect, the fluorescence spectra were obtained with commercial humic acids and a model protein (bovine serum albumin [BSA]). It seemed that the commercial humic acids had a strong quenching effect on the excitation-emission spectrum of BSA, reducing or even eliminating the protein peak in the 2D-fluorescence map. This loss of fluorescence intensity is called quenching and resulted from the interaction of the excited molecule of protein with the humic acids, whatever the nature of the competing

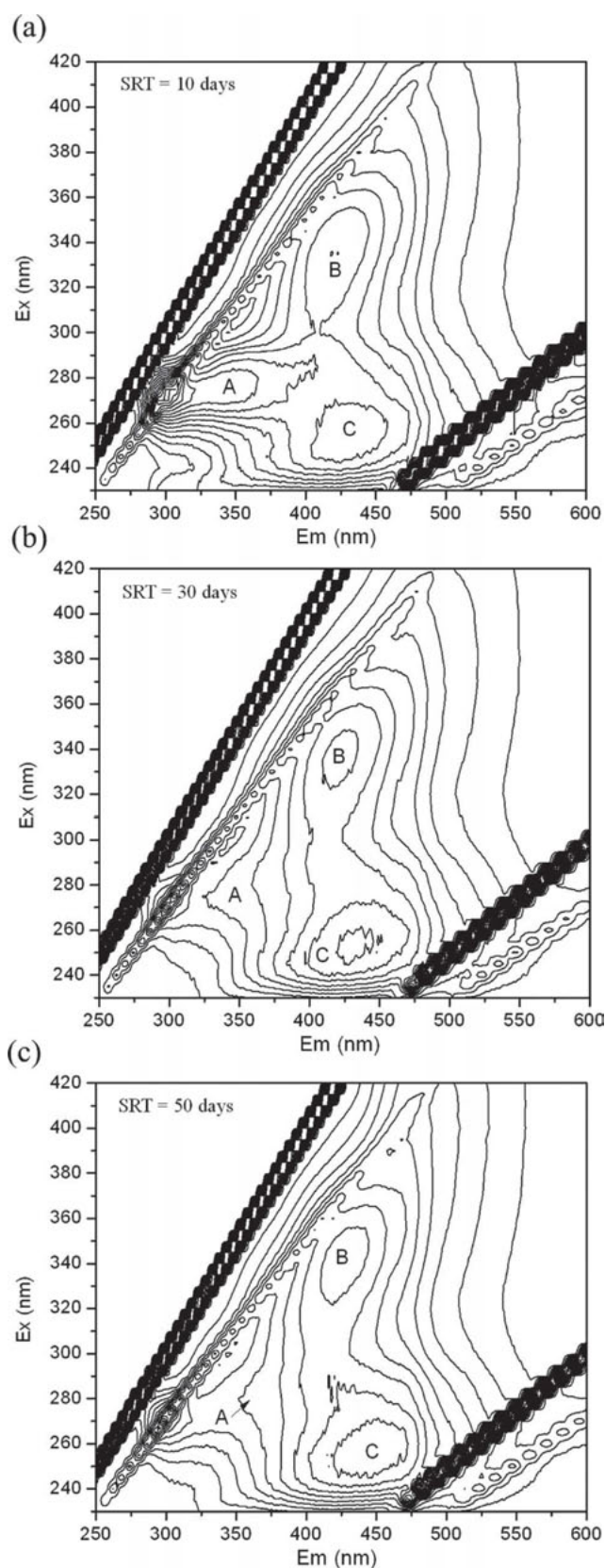


Fig. 3. EEM fluorescence spectra of SMP in MBR-MC system. SRT = (a) 10 d; (b) 30 d; (c) 50 d.

intermolecular process. Previous study [20] also found that humic acids had a strong effect on the fluorescence spectrum of BSA, reducing the aromatic protein-like substances peak in the fluorescence map. These results suggested that quantitative determination of proteins in such complex media was not feasible with fluorescence in view of the interference of other compounds likely to be present in the system, although this effect might have been amplified by the fact that the humic acids concentration used in this experiment was much higher than it was likely to be present in real samples. Nevertheless, quenching effect in protein measurements, and peak overlapping in the humic-like compounds region has to be considered since it caused interferences in SMP analyses by fluorescence.

To overcome this shortage, the principal components analysis (PCA) and multivariate curve resolution method based on alternating least squares (MCR-ALS) can be used to determine the number of fluorophores present in the SMP sample which some of them have binding site properties, their excitation and emission spectra and the corresponding quenching profiles. Alternatively, it was possible to use size exclusion chromatography to separate different fractions as a function of molecular weight and then apply 2D-fluorescence to characterize each fraction [21]. The application of these techniques enabled monitoring the proteins in a deterministic way using fluorescence, which was not discussed in this study and would be primary focus in the following research.

### 3.5. Application of RSM for SMP prediction

On the basis of RSM, an empirical relationship between the response and the independent variables is expressed by the following quadratic model:

$$\begin{aligned} \text{SMP production (Y)} = & 70.42 - 1.02X_1 - 0.032X_2 \\ & - 1.78X_3 - 15.64X_4 + 0.00025X_1X_2 + 0.00010X_1X_3 \\ & + 0.052X_1X_4 - 0.0096X_2X_3 + 0.080X_2X_4 - 0.023X_3X_4 \\ & + 0.014X_1^2 - 0.0083X_2^2 + 0.050X_3^2 + 4.68X_4^2 \end{aligned} \quad (5)$$

The adequacy of the model was justified through analysis of variance (ANOVA), and the ANOVA for the quadratic model is summarized in Table 4. There was a high correlation between the observed and predicted value as shown by closeness between  $R^2$  (0.905) and adjusted  $R^2$  (0.794), indicating that the regression model provided an excellent explanation of the relationship between the independent variables and the response. The  $F$  statistic of 8.159 was found much greater than the  $F_{0.005,14,16}$  (4.02), and the low  $p$ -value (0.000) also confirmed the adequacy of the model.

Simultaneously, the significance of each coefficient was determined by applying  $t$ -test, wherein larger  $t$ -values and smaller  $p$ -values indicated a greater level. In this case, significant factors for the response SMP were linear terms of SRT ( $X_1$ ), temperature ( $X_3$ ) and aeration rate ( $X_4$ ), with  $p$ -values of 0.000, 0.000 and 0.002, respectively. All above-mentioned factors showed synergistic

Table 4

Coded coefficients of quadratic models for the SMP production and the ANOVA evaluation of the unreduced models

Source	Value	Degree of freedom	Standard deviation	$t$ value	$p$ value
Intersection	70.42	1	8.475	8.310	0.000 <sup>1</sup>
$X_1$	-1.02	1	0.216	-4.728	0.000 <sup>1</sup>
$X_2$	-0.032	1	0.882	-0.036	0.972
$X_3$	-1.78	1	0.373	-4.781	0.000 <sup>1</sup>
$X_4$	-15.64	1	4.056	-3.857	0.002 <sup>1</sup>
$X_{12}$	0.00025	1	0.012	0.022	0.983
$X_{13}$	0.00010	1	0.005	0.022	0.983
$X_{14}$	0.052	1	0.058	0.906	0.383
$X_{23}$	-0.0096	1	0.019	-0.496	0.629
$X_{24}$	0.08	1	0.232	0.345	0.736
$X_{34}$	-0.023	1	0.097	-0.237	0.817
$X_{11}$	0.014	1	0.003	5.694	0.000 <sup>1</sup>
$X_{22}$	-0.0083	1	0.040	-0.207	0.839
$X_{33}$	0.050	1	0.007	7.100	0.000 <sup>1</sup>
$X_{44}$	4.68	1	1.004	4.660	0.001 <sup>1</sup>

$R^2 = 0.905$ , Adj- $R^2 = 0.794$ ,  $F = 8.159$ ,  $p = 0.000$ .

<sup>1</sup>Means highly significant.



effect in the minimization of SMP production. Additionally, the quadratic terms of SRT ( $X_1$ ), temperature ( $X_3$ ) and aeration rate ( $X_4$ ) had positive effect on SMP response ( $p$ -values of 0.000, 0.000 and 0.001). Although the first order effect showed that increase in these variables,  $X_1$ ,  $X_3$  and  $X_4$ , was adverse for SMP minimization. The simultaneous increase in  $X_1^2$ ,  $X_3^2$  and  $X_4^2$  favored for the SMP production, as shown by the second-order effect of the last term in the polynomial expression. The interaction effect of other independent variables had no significant ( $p > 0.05$ ) influence on the SMP production, indicating that the effect of these terms on the response model was not statistically significant at the 95% confidence level. The insignificant model terms were removed to ultimately produce a new and improved experimental model as given in Eq. (6).

$$\text{SMP production (Y)} = 68.50 - 0.96X_1 - 1.90X_3 - 14.06X_4 + 0.014X_1^2 + 0.050X_3^2 + 4.75X_4^2 \quad (6)$$

The ANOVA analysis of the reduced model equation after eliminating the insignificant terms for SMP production is shown in Table 5. The  $R^2$  and adjusted  $R^2$  were 0.866 and 0.826 respectively, indicating an excellent agreement between the experimental and predicted SMP production. In addition, the model resulted in an  $F$ -value of 21.61 with an extremely low  $p$ -value (0.000) for SMP production, implying that the model is highly significant and adequate for the response variables.

Using the reduced quadratic model, response surface graphs were plotted with one variable kept constant at the zero-level value, and the other two allowed varying over the experimental ranges. Fig. 4 shows the response contour of the effect with different parameters combinations, namely SRT, temperature and aeration rate on the SMP content, in order to gain a better understanding of the interaction effect of those flotation variables. A circular contour plot showed that the

interactions between the corresponding variables were negligible, whereas an elliptical or saddle pattern indicated significant interactions.

Fig. 4(a) shows the 3D response surface relationship between SRT and temperature on the SMP production at the centre level of aeration rate ( $X_4$ ). The SMP production decreased as the temperature increased from 8°C to 21.6°C, whereas the production increased as the temperature values increasing from 21.6°C to 32°C. At low temperature, the biomass was under stress and produced more SMP to protect cells, and the bacterial metabolism slowed down, which led to a slower rate of substrate and SMP degradation. Additionally, more SMP was observed at high temperature because of the increase metabolic activity of microbes. Fig. 4(b) displays the 3D and contour plot between SRT and aeration intensity at temperature (20°C). From Fig. 4(b), it can be conjectured that the best operational conditions were likely around the center levels of SRT and aeration intensity. The sensitive response to the reaction SRT was likely associated with the concentration of UAP and BAP produced in the MBR system. The UAP concentration decreased as the SRT was increased, while the BAP concentration increased as the SRT was extended [15]. Hence, a minimum SMP concentration was existed for an optimal SRT which was about 34 d for this model results.

Fig. 4(c) demonstrates the 3D response surface which is constructed to show the most important two variables (temperature and aeration rate) in the production of SMP with the SRT set at 30 d. The trend for temperature was the same as in Fig. 4(a). Increasing the aeration rate from 0.2 to 1.5 m<sup>3</sup> h<sup>-1</sup> decreased the SMP production, and after aeration rate of 1.5 m<sup>3</sup> h<sup>-1</sup>, the SMP production increased. At low aeration rate, a lower DO concentration was generated, suggesting the shortage of DO as an oxygen source for mineralization of SMP. The subtle increase of the SMP concentration in response to increased aeration rate from 1.5 to 2.2 m<sup>3</sup> h<sup>-1</sup> can be explained by the erosion of floc-associated EPS coupled

Table 5

Coded coefficients of quadratic models for the SMP production and the ANOVA evaluation of the reduced models

Source	Value	Degree of freedom	Standard deviation	$t$ value	$p$ value
Intersection	68.50	1	3.618	18.934	0.000 <sup>1</sup>
$X_1$	-0.96	1	0.134	-7.194	0.000 <sup>1</sup>
$X_3$	-1.90	1	0.247	-7.715	0.000 <sup>1</sup>
$X_4$	-14.06	1	2.175	-6.462	0.000 <sup>1</sup>
$X_{11}$	0.014	1	0.002	6.656	0.000 <sup>1</sup>
$X_{33}$	0.050	1	0.006	8.281	0.000 <sup>1</sup>
$X_{44}$	4.75	1	0.869	5.462	0.000 <sup>1</sup>

$R^2 = 0.866$ , Adj- $R^2 = 0.826$ ,  $F = 21.61$ ,  $p = 0.000$ .

<sup>1</sup>Means highly significant.



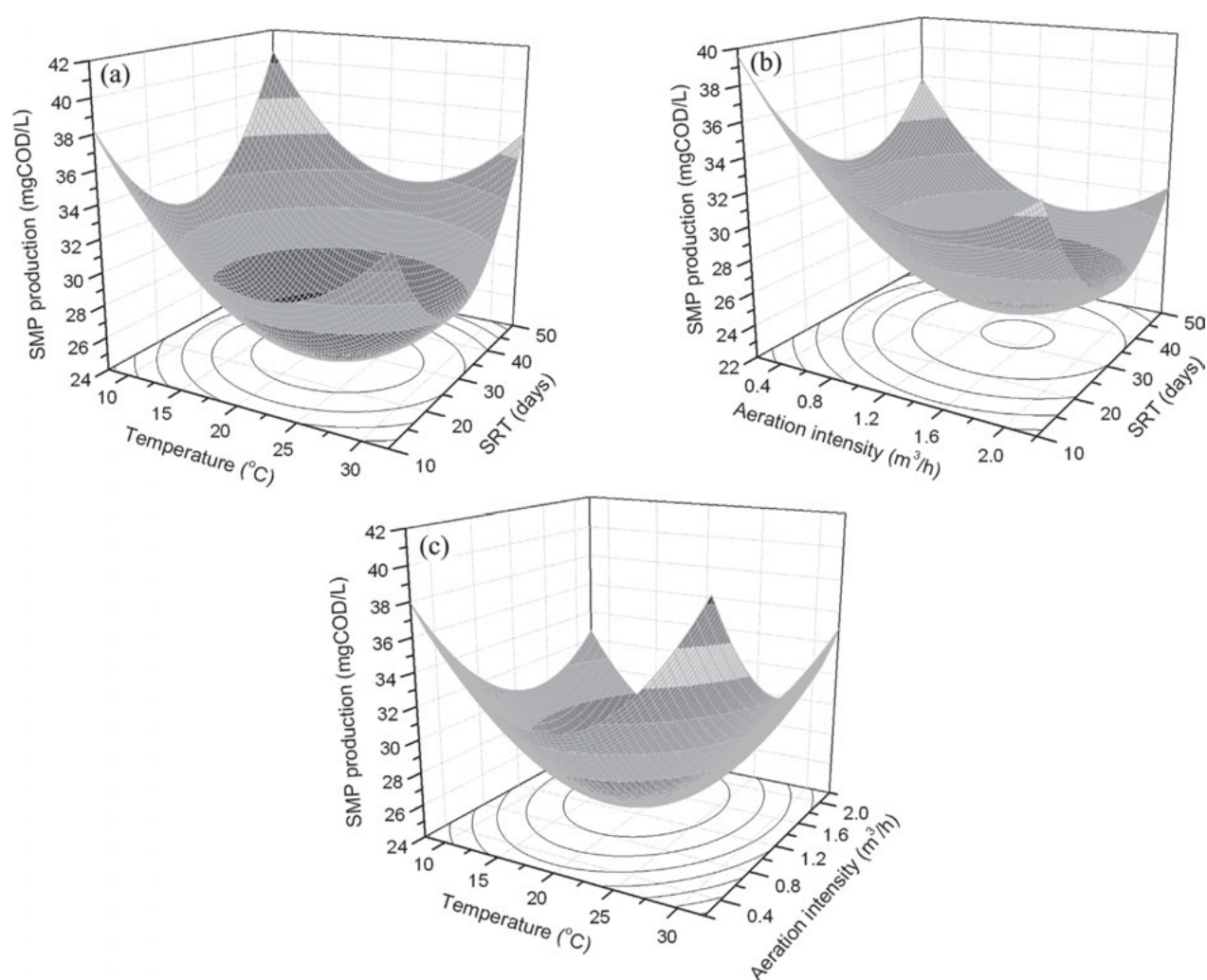


Fig. 4. (a) 3D response surface: interactive effects of varied SRT and temperature at aeration intensity 1.2 m³ h⁻¹; (b) 3D response surface: interactive effects of varied SRT and aeration intensity at temperature 20°C; (c) 3D response surface: interactive effects of varied temperature and aeration intensity at SRT 30 d.

with relative slow degradation of the released soluble SMP. That was possibly why there was an optimum at around aeration rate 1.5 m³ h⁻¹.

One of the main aims in this study was to find the optimum process parameters to minimize the SMP production from the developed mathematical model equation. The quadratic model equation was optimized by setting the partial derivatives of Eq. (6) to zero with respect to the corresponding variables, obtaining the optimal parameters of SRT, temperature and aeration intensity. Regarding the effect of HRT, the SMP production reached a minimum at the longest time of 13 h which was the upper limit of HRT designed in this study and might result in a little lower production with an even longer time. However, the higher HRT surely resulted in severe energy consumption and promoted the release of

colloids and solutes from the microbial flocs to the bulk solution which might increase the SMP production and thus intensify the membrane fouling. Incorporated with the simulation results of the unreduced model (Eq. (5)), an optimum HRT of 10 h was suggested from the SMP production and economic point of view. Therefore, the optimum SMP production conditions were obtained at 33 d of SRT, 10 h of HRT, 20°C of temperature, 1.4 m³ h⁻¹ of aeration rate with a predicted SMP production of 24.0 mg l⁻¹. In order to confirm these results, three independent, complementary experiments were carried out under the optimal condition. From the presented data (Table 6), the obtained experimental SMP production was very close to the predicted value estimated ( $23.6 \pm 1.3$  mg l⁻¹). Therefore, the model was useful for predicting SMP production as well as optimization of the experimental conditions.

Table 6  
Results of confirmation experiments

Trail	SRT (d)	HRT (h)	Temperature (°C)	Aeration rate (m <sup>3</sup> h <sup>-1</sup> )	SMP concentration (mg l <sup>-1</sup> )	
					Measured	Simulated
1					22.3	
2	33	10	19	1.5	24.9	23.9
3					23.5	

#### 4. Conclusions

Three identical submerged MBR-MCs were operated with synthetic wastewater to investigate differences in characteristics of SMP at different SRTs. Accumulation of SMP in the MBR-MCs was more pronounced at short and long SRTs. The profile of the MWD showed that the SMP had a wide spectrum of molecular weight and the SMP with a MW higher than 10 kDa accounted for the highest amount. As the SRT was extended from 10 to 50 d, the percentage of higher MW (>10 kDa) obviously increased accompanied by a decrease in the percentage of low MW. The excitation–emission matrix fluorescence spectroscopy showed that SMP had three similar peak locations regardless of SRT and the quenching effect of humic-like substance on protein could not be neglected. The response surface methodology design was used to determine the effects of SRT, HRT, temperature and aeration rate on SMP generation, and to optimize the best operating conditions for SMP production. Satisfactory predicted equations were developed and the production of SMP could be minimized (23.9 mg l<sup>-1</sup>) under the following conditions: an SRT of 33 d, an HRT of 10 h, a temperature of 19°C and an aeration rate of 1.5 m<sup>3</sup> h<sup>-1</sup>, respectively.

#### Acknowledgements

This study was supported by the National High-tech R&D Program (863 Program) of China (Contract No. 2007AA06Z348) and the State Key Laboratory of Urban Water Resource and Environment, Harbin Institute of Technology (No. 2011DX01).

#### References

- [1] M. Turan, O. Ozdemir, A.Z. Turan, O. Ozkan, H. Bayhan and E. Aykar, Performance of a flat-sheet submerged membrane bioreactor during long-term treatment of municipal wastewater, *Desalin. Water Treat.*, 26 (2011) 53–56.
- [2] N. Xue, J. Xia and X. Huang, Fouling control of a pilot scale self-forming dynamic membrane bioreactor for municipal wastewater treatment, *Desalin. Water Treat.*, 18 (2010) 302–308.
- [3] S. Yang, F. Yang, Z. Fu and R. Lei, Comparison between a moving bed membrane bioreactor and a conventional membrane bioreactor on organic carbon and nitrogen removal, *Bioresour. Technol.*, 100 (2009) 2369–2374.
- [4] K.K. Ng, C.F. Lin, S.K. Lateef, S.C. Panchangam, P.K.A. Hong and P.Y. Yang, The effect of soluble microbial products on membrane fouling in a fixed carrier biological system, *Sep. Purif. Technol.*, 72 (2010) 98–104.
- [5] E. Bouhabila, R. Ben Aim and H. Buisson, Fouling characterisation in membrane bioreactors, *Sep. Purif. Technol.*, 22–23 (2001) 123–132.
- [6] S. Rosenberger, H. Evenblij, S. Te Poele, T. Wintgens and C. Laabs, The importance of liquid phase analyses to understand fouling in membrane assisted activated sludge processes—six case studies of different European research groups, *J. Membr. Sci.*, 263 (2005) 113–126.
- [7] D.J. Barker and D.C. Stuckey, A review of soluble microbial products (SMP) in wastewater treatment systems, *Water Res.*, 33 (1999) 3063–3082.
- [8] X.M. Wang and T.D. Waite, Retention of soluble microbial products in submerged membrane bioreactors, *Desalin. Water Treat.*, 6 (2009) 131–137.
- [9] Y. Tian, L. Chen, S. Zhang and S. Zhang, A systematic study of soluble microbial products and their fouling impacts in membrane bioreactors, *Chem. Eng. J.*, 168 (2011) 1093–1102.
- [10] H.F. Zhang, B.S. Sun, X.H. Zhao and J.M. Sun, Membrane fouling caused by soluble microbial products in an activated sludge system under starvation, *Desalin. Water Treat.*, 1 (2009) 180–185.
- [11] APHA, Standard Methods for the examination of water and wastewater 20th ed, Am. Public. HLTH Assoc. Washington, DC, (1998).
- [12] M. Dubois, K. Gilles, J. Hamilton, P. Rebers and F. Smith, Colorimetric method for determination of sugars and related substances, *Anal. Chem.*, 28 (1956) 350–356.
- [13] O. Lowry, N. Rosebrough, A. Farr and R. Randall, Protein measurement with the Folin phenol reagent, *J. Biol. Chem.*, 193 (1951) 265–275.
- [14] W. Xie, B. Ni, R. Zeng, G. Sheng, H. Yu, J. Song, D. Le, X. Bi, C. Liu and M. Yang, Formation of soluble microbial products by activated sludge under anoxic conditions, *Appl. Microbiol. Biotechnol.*, 87 (2010) 373–382.
- [15] Y. Tian, L. Chen and T. Jiang, Characterization and modeling of the soluble microbial products in membrane bioreactor, *Sep. Purif. Technol.*, 76 (2011) 316–324.
- [16] J. Ji, J. Qiu, F.-s. Wong and Y. Li, Enhancement of filterability in MBR achieved by improvement of supernatant and floc characteristics via filter aids addition, *Water Res.*, 42 (2008) 3611–3622.
- [17] W. Lee, S. Kang and H. Shin, Sludge characteristics and their contribution to microfiltration in submerged membrane bioreactors, *J. Membr. Sci.*, 216 (2003) 217–227.
- [18] B.J. Ni, R.J. Zeng, F. Fang, W.M. Xie, G.P. Sheng and H.Q. Yu, Fractionating soluble microbial products in the activated sludge process, *Water Res.*, 44 (2010) 2292–2302.

- [19] W. Chen, P. Westerhoff, J. Leenheer and K. Booksh, Fluorescence excitation- emission matrix regional integration to quantify spectra for dissolved organic matter, *Environ. Sci. Technol.*, 37 (2003) 5701–5710.
- [20] C. Kobblerø, K. Keiding, K.L. Larsen and P. Halkjær Nielsen, Quenching effects in the application of multi-channel fluorescence in activated sludge suspended solids, *Water Res.*, 42 (2008) 2449–2456.
- [21] N. Her, G. Amy, D. McKnight, J. Sohn and Y. Yoon, Characterization of DOM as a function of MW by fluorescence EEM and HPLC-SEC using UVA, DOC, and fluorescence detection, *Water Res.*, 37 (2003) 4295–4303.